LOW-SPEED AERODYNAMIC CHARACTERISTICS OF A BUSEMANN-TYPE SILENT SUPERSONIC BIPLANE

Hiromitsu Kawazoe*, Shinji Abe*, Takashi Matsuno*,
Goji Yamada* and Shigeru Obayashi**
*** Dept. of Mech. and Aerospace Eng., Tottori University, Tottori, JAPAN,**
**** Institute for Fluid Science, Tohoku University, Sendai, JAPAN**

Keywords: *Aerodynamics, Supersonic biplane, Low speed characteristics, Wind tunnel*

Abstract

Aerodynamic performances of three Busemann-types of silent supersonic biplanes were studied by a low-speed wind tunnel experiment. These wings have the plane configurations of the front-side tapered, the rear-side tapered and the both-side tapered shape. Lift, drag and pitching moment of the biplanes were measured in the both cases of their pitching motion and the static conditions by using the compact force balance developed in the authors' laboratory of Tottori University.

All of the three biplanes show the same C_L characteristic as a thin wing at a low angle of attack. The biplane with the front-side tapered shape has the larger lift inclination in the attack angle from eight to seventeen degrees than the other biplanes and indicates clearly the stall phenomena at the attack angle of seventeen degrees. It was found that the front-side tapered wing generates leading edge separation vortices just like a delta wing and the occurrence of the vortex breakdown is the reason for the stall.

The dynamic characteristics of lift, drag, and pitching moment in their pitching motions drew hysteresis loops around the static results with an angle of attack. The aerodynamic performances with the low frequency pitching of 0.5 Hz approaches closer to the static ones than the results of the high pitching, 1.0 Hz. It is based on the fact that the airflow around the biplane cannot follow immediately the motion of the biplane. Furthermore, the longitudinal static stability of the three biplanes became worse in the higher pitching motion.

1 Introduction

A Busemann-type biplane [1],[2] is known as a wing for a supersonic flight vehicle owing to its low drag performance, because the wing utilizes beneficial interference between shock and expansion waves coming from the upper and the lower wings of the biplane. Furthermore, the biplane aircraft will be also expected as a silent supersonic flight vehicle since the shock waves at the leading and the trailing edges will be drastically weakened owing to the interaction of the shock and the expansion waves. It results in the reduction of the strength of the N-shape pressure wave at the ground.

On the other hand, a supersonic Busemann-type biplane will not be able to avoid taking off and landing at a low speed, in the time of which the supersonic aircraft must have a large angle of the attack to obtain a sufficient lift.

MISORA (Institute of Fluid Science, Tohoku University)

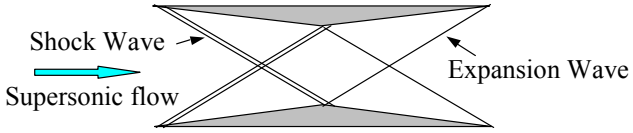

Fig.1 Busemann-type supersonic vehicle, MISORA, and its silent mechanism.

The author of the article, Obayashi, has proposed this type of a silent biplane as shown in Fig.1, the name of which is MISORA [3]. He and his coworkers have conducted and carried out the research on the biplane at the supersonic flight by the numerical procedure in such the conditions as the entrance from subsonic to supersonic [4] and the off-design flight [5]. The experimental study have tried with a ballistic range [6], and been in progress by the free flight test.

The research for the low-speed flight like a landing and taking-off have been also conducted [7], [8]. The researches on the low-speed performance of the Busemann-type biplane have been conducted by the low speed wind tunnel test at Tottori University, especially targeting at unsteady flight conditions. In this study the dynamic characteristics of a silent supersonic biplane in pitching motion as well as the static condition were investigated. The pitching motion was realized by the parallel-type manipulator designed and manufactured by the author [9].

The objective of the current study is to explore the performances of three types of a Busemann-type biplane in a low speed wind tunnel as shown in Fig.2. The characteristics of these biplanes were investigated by measuring the longitudinal three-component of the aerodynamic force and moment by using the compact force balance which was also developed by the author [9].

2 Experimental Apparatus and Method

The schematic diagram of the experimental setup in the wind tunnel is illustrated in Fig.2, which shows the biplane under pitching condition. The pitching motion was undertaken by using the parallel-type manipulator equipped with six stepping motors. The manipulator can make the biplane an arbitrary motion owing to the six degrees of freedom equipped with the manipulator. The pitching frequency was set in 0.5 and 1.0 Hz. The experimental conditions is listed in Table 1. On the other hand, the static condition of a biplane was also investigated for the comparison with the dynamic performances at the attack angle from 0 to 35 degrees.

Figure 3 shows the three types of the Busemann-type biplanes explored in the research, that is front-side, rear-side and both-side tapered biplane models. They have the same maximum root chord of 83.4mm and the wingspan of 200mm. The other specifications of the biplane are listed in Table 2. On the other hand, the monoplane models were also investigated to compare with those of the biplanes, which were composed of the lower wing of these biplanes as shown in Fig.3 (b).

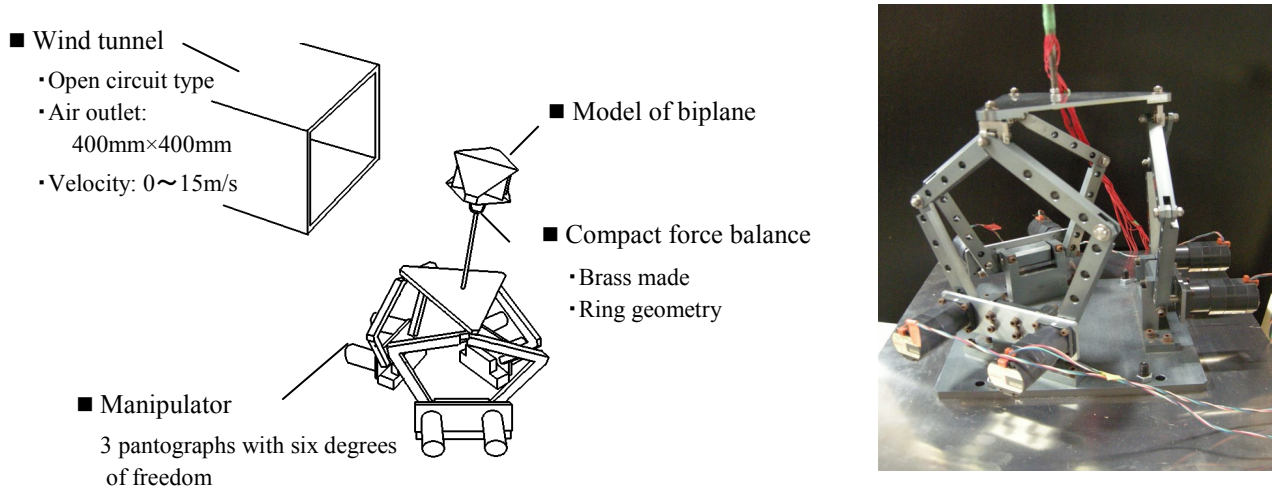

Fig.2 Experimental setup and the manipulator to make a pitching motion of biplanes.

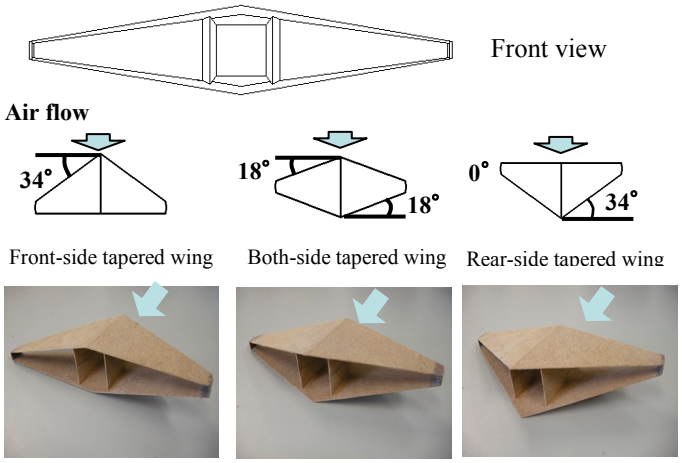

(a) Three types of biplanes

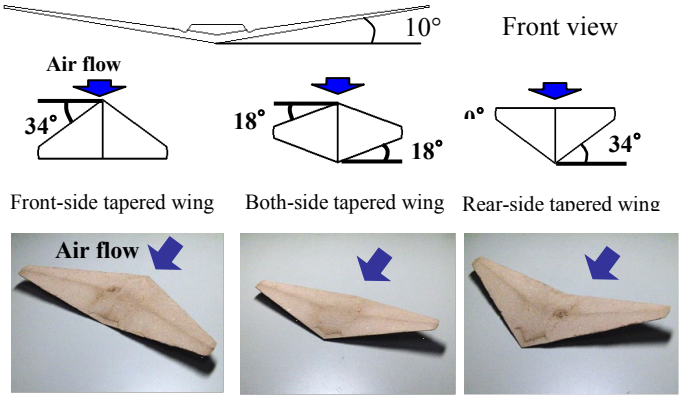

(b) Three types of monoplanes (lower wing of (a))

Fig.3 Biplane and mono-plane models.

Table 1 Experimental conditions

Attack angle : α	0~35° (static)
	10°±10° (pitching)
Pitching frequency	0.5Hz, 1.0Hz
Strouhal number	0.0042, .0084
Free stream velocity	10m/s
Reynolds number	5.1×10^4

Table 2 Biplane model specifications

Max. chord length	83.4 mm
Wing span	200 mm
Wing area	0.01 m^2
Aspect ratio	4.0
Wing taper ratio	0.2

The aerodynamic characteristics of lift, drag and pitching moment of the biplanes and the monoplanes were measured by a compact force balance, the weight of which is 5.6g. It was also developed by the author [9] and the specifications are shown in Fig.4. The strain gage pasted at the location of 39.6 degrees from the centerline of the force balance is for drag

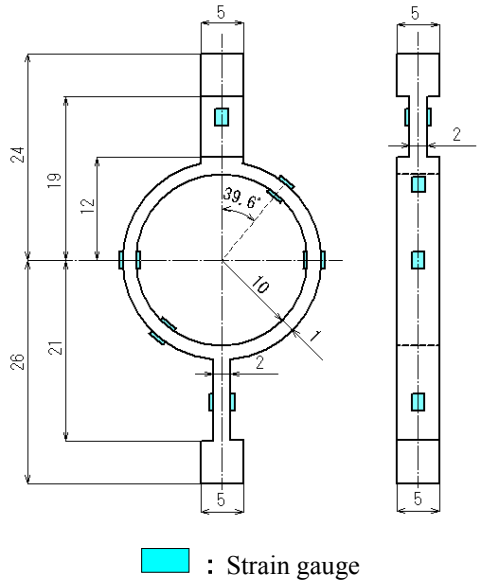

Fig.4 Compact four-component force balance.

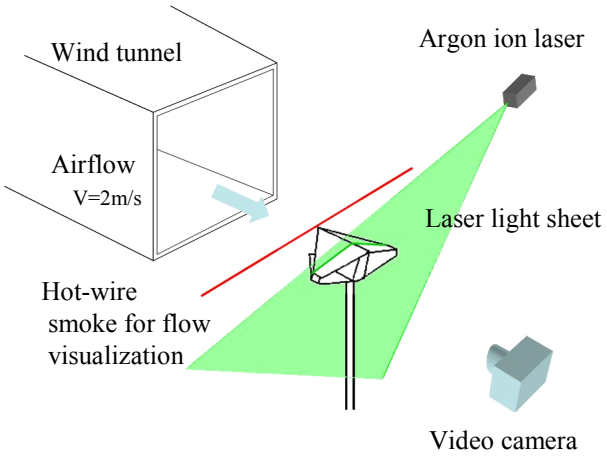

Fig.5 Flow visualization by a laser sheet.

measurement and that of 90 degrees is for lift. The strains at the both locations are not interactive each other.

The airflow just above the upper wing of the biplane was visualized by the laser light sheet method as shown in Fig.5. It was planned to understand the results of the aerodynamic characteristics measured by the force balance and to ascertain a numerical prediction. In the visualization research, the velocity of the free stream of the wind tunnel was reduced 10m/s to 2m/s to prevent smoke cloud from rapid diffusing. It was considered the essence of the flow could be caught at the low speed condition. Furthermore, CFD analysis was also carried out to confirm the airflow behavior passing through the biplane in the static condition.

3 Results and Discussions

Lift versus an angle of the attack in the static condition is shown in Fig.6. The lift of the all biplanes increases linearly at low angle of the attack and the inclination is just similar to that of a general thin wing. In this linear increase region the lift, $C_{L,}$ of the both-side tapered biplane has the maximum value over 0.8 at α =8 degrees. The rear-side and the both-side tapered biplanes have the similar C_L tendency to a thin wing at a higher angle of the attack. The lift of the rear-side tapered biplane, although, becomes larger than the both-side biplane at the attack angle higher than 15 degrees on the contrary to the liner C_L region.

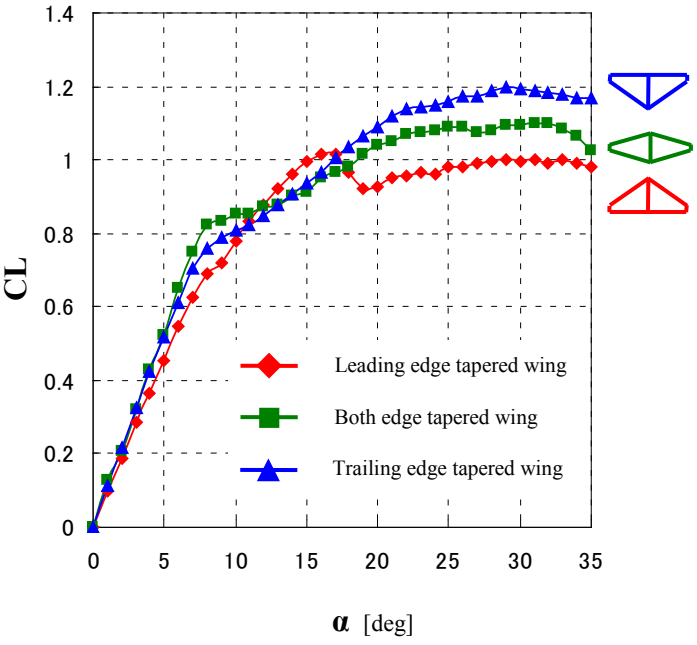

Fig.6 Lift versus attack angle in static condition.

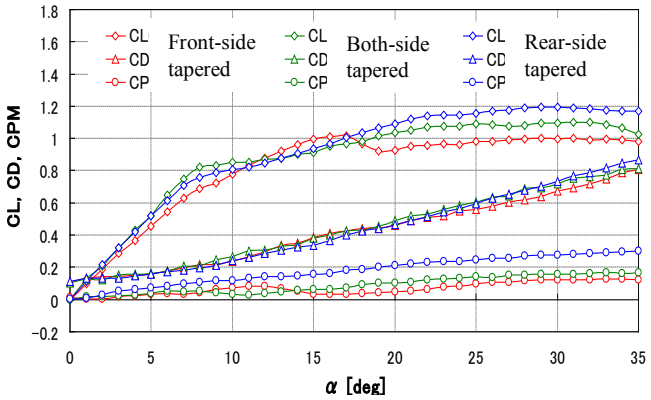

Fig.7 Lift, drag and pitching moment of the biplanes in the static condition.

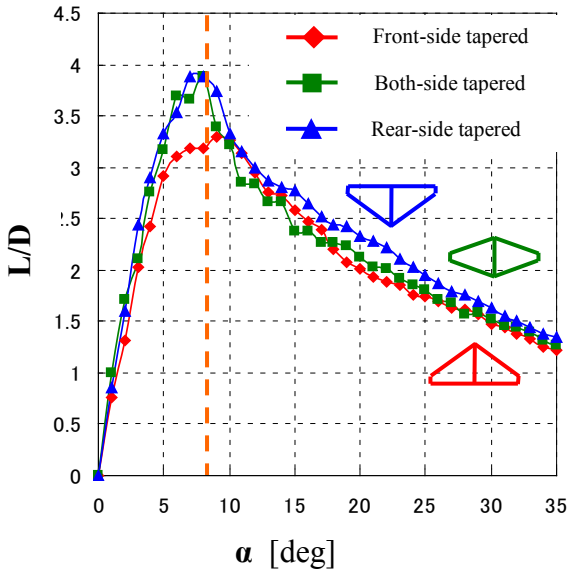

Fig.8 Ratio of lift to drag with an angle of attack.

The lift of the front-side tapered biplane, on the other hand, gives the second larger increase of C_L after the linear region, namely over α=8 degrees. Furthermore, the C_L curve made the sudden drop at α=17 degrees clearly, which is the same lift performances as a delta wing besides the occurrence at the lower angle of the attack. Such the decrease of lift occurred over thirty degrees in the rear-side and the both-side tapered biplanes.

The drag, C_D, and the pitching moment, C_{PM}, versus an angle of the attack are sown in Fig.7. The front-side and the both-side tapered biplanes have a negative slope of $\delta C_{PM}/\delta\alpha$ and it is a suggestive characteristic for a longitudinal static stability in these biplanes. However, the rear-side tapered biplane has a positive $\delta C_{PM}/\delta\alpha$ in the whole region of an angle of the attack.

The ratio of lift to drag for the biplanes is shown in Fig.8. The L/D of the front-side tapered biplane becomes the worst, because the lower lift than the other biplanes at the linear C_L region in Fig.6 and the almost same drag performances in Fig.7 were appeared in a small angle of the attack for the maximum L/D. The rear-side tapered biplane gave the best result for L/D performance, and the maximum value is 3.9 at the attack angle near 8 degrees. The both-side tapered biplane has the similar L/D to the rear-side tapered wing, especially at a low angle of the attack.

The lift for the monoplane models is indicated in Fig.9, where the reference area for C_L is the same as the biplane models. As the

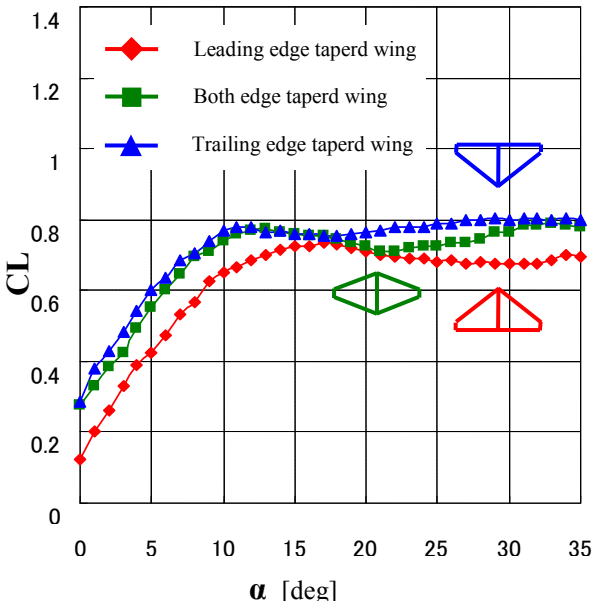

Fig.9 Lift of the monoplanes with attack angle.

results, these monoplanes' lift became lower than the biplane models properly and the maximum C_L are about 0.8 of the rear-side and the both-side tapered monoplanes. The front-side tapered monoplane marked the worst value because the sweep-back leading edge should be not effective for a low-speed flight at all.

The aerodynamic performance of the front-side tapered biplane in pitching motion with the frequency of 0.5Hz is shown in Fig.10. The static result is also plotted in the figure. The blue line is the result for the pitch-up motion of the biplane which is indicated by the symbol + α, and the red one is for the case of the pitch-down motion with the symbol of – α. The large hysteresis of C_L can be recognized near the stall angle of α=17 degrees, and the hysteresis loop draw an shape of Arabic figure eight in detail. The static result exists just in the middle of this Arabic figure eight hysteresis loop.

Figure 11 shows the C_L, C_D and C_{PM} for the pitching motion in the both cases of the pitching frequency of 0.5 and 1.0Hz. The static

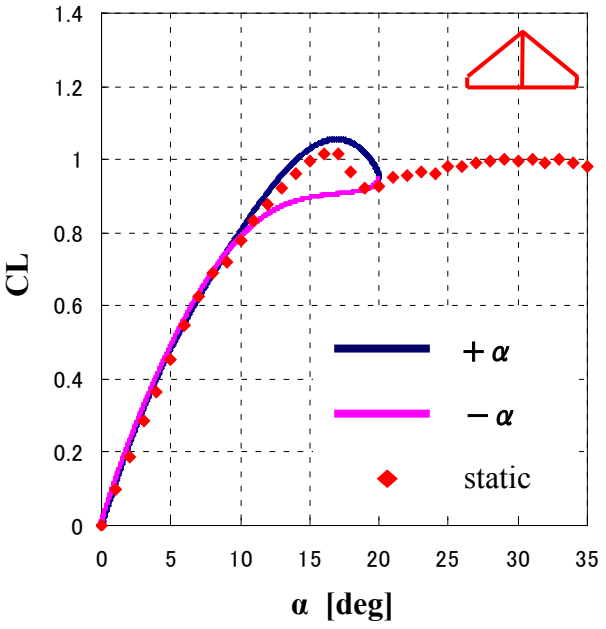

Fig.10 Dynamic CL performance of the front-side tapered biplane.

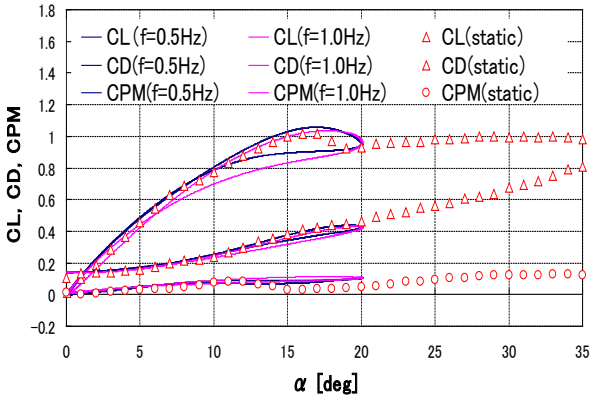

(a) Front-side tapered biplane

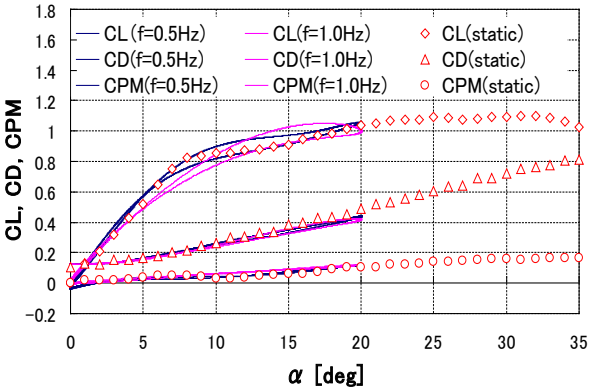

(b) Both-side tapered biplane

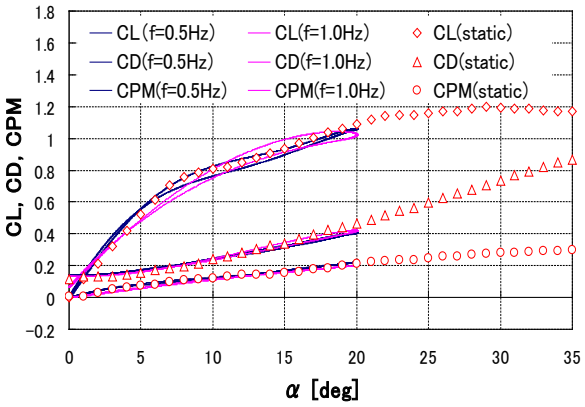

(c) Rear-side tapered biplane

Fig.11 Dynamic performance of the biplanes.

results are also plotted in the figure. The 0.5Hz results are closer to the static results than the 1.0Hz ones. The reason is considered that the flow field around the pitching biplanes with the frequency of 0.5Hz follows better than those of the high-frequency pitching motion. Owing to

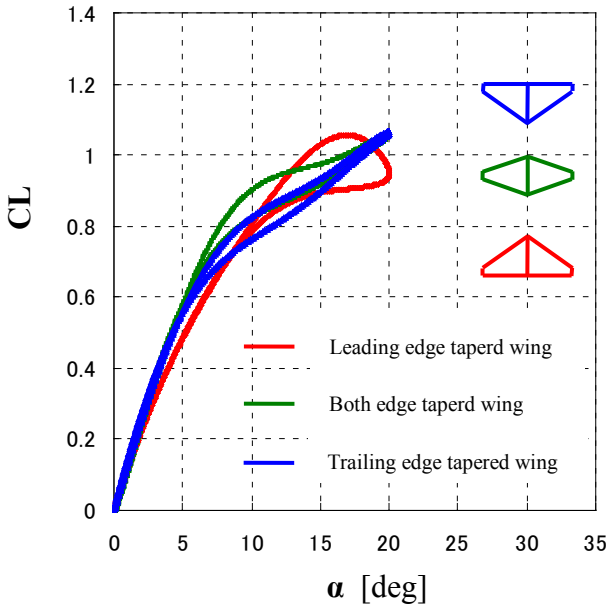

(a) Pitching frequency of 0.5Hz

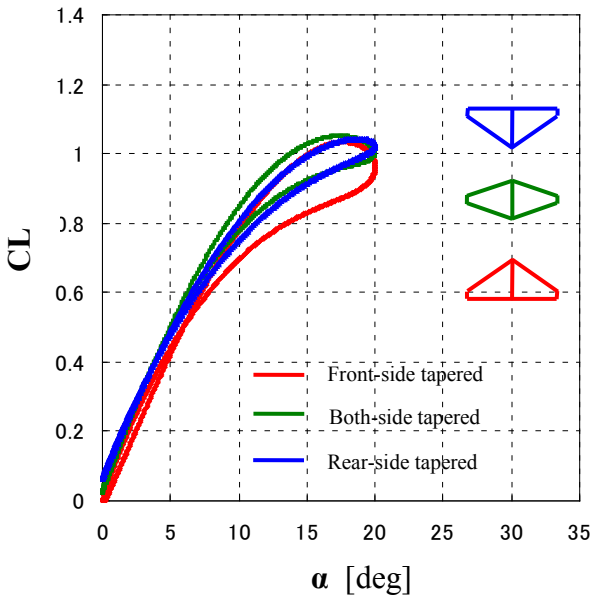

(b) Pitching frequency 1.0Hz

Fig.12 Lift variation in the pitching motion.

the delay of the flow following the pitching motion at the frequency of 1.0Hz, the stall of the front-side and the other two tapered biplanes were delayed compared with the static and 0.5Hz pitching results.

Figure 12 shows the comparison of lift in the pitching motion for three types of the biplanes, (a) for 0.5 Hz and (b) for 1.0Hz. The C_L in the 0.5Hz pitching motion became an individual hysteresis loop for each biplane, which kept the peculiarity of the static result. On the other hand, the C_L curve at high frequency condition of 1.0Hz became a mutual hysteresis loop for the three biplanes. It is due to the flow field being worse subordinate to the wing motion.

The airflow was investigated by the numerical simulation to discuss the results mentioned above. Because of the difficulty to simulate in pitching motion the static condition for an representative angle of the attack, namely α=10 degrees, was targeted in the research. The streamlines and the pressure distributions on the upper and the lower wing surfaces are shown in Fig.13 in the case of the front-side tapered biplane. The similar results for the both-side and the rear-side tapered biplanes are indicated in Figs.14 and 15, respectively. It is obvious that an attached flow should be generated on the lower surface of the upper and the lower wings in all of the biplanes and the resultant pressure distributions became similar except the effect of the tapered edge location and the projected surface location for expansion waves.

However, the pressure on the upper surfaces is considered to have a great effect to an aerodynamic performance. Therefore, the flow fields on the upper surface of the wings are indicated in Figs.13-15, the left figure for the upper and the right for the lower. On the lower wing surface, the high pressure region generated around the front edge near the root chord and the low pressure area was formed along the leading edge as well as the centerline of the chord in the span direction where the airflow

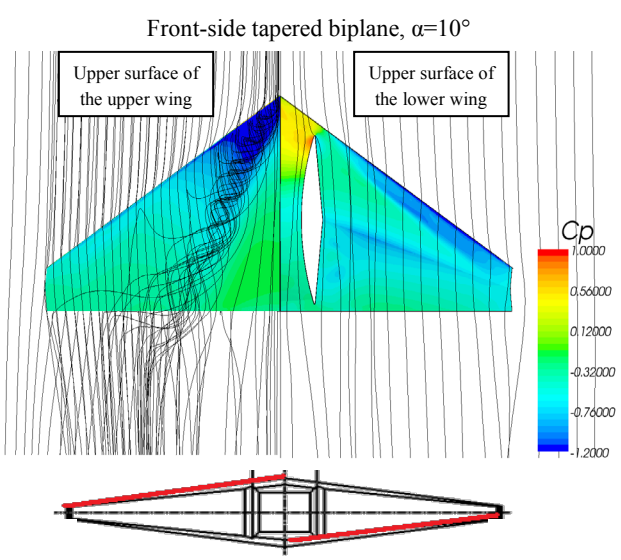

Fig.13 Streamlines and pressure distributions of the front-side tapered biplane, α=10 degrees.

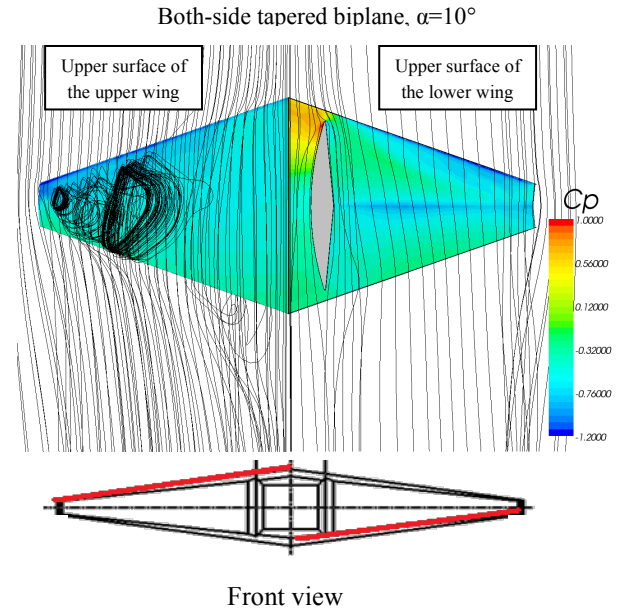

Fig.14 Streamlines and pressure distributions of the both-side tapered biplane, α=10 degrees.

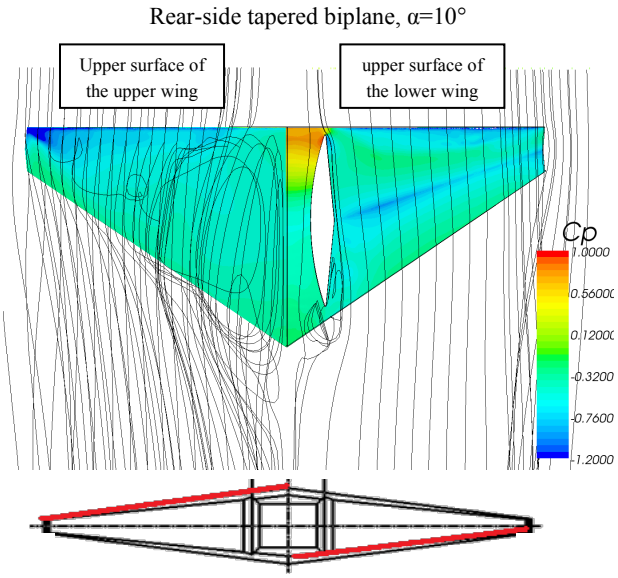

Fig.15 Streamlines and pressure distributions of the rear-side tapered biplane, α=10 degrees.

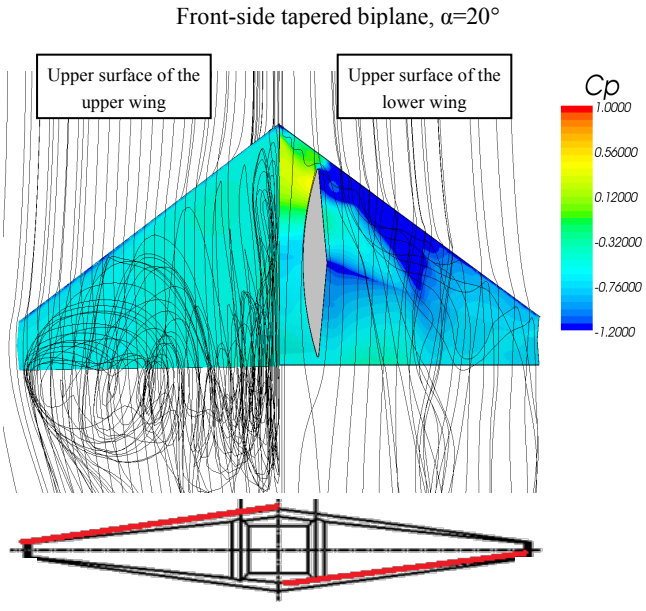

Fig.16 Streamlines and pressure distributions of the front-side tapered biplane, α=20 degrees.

accelerated owing to the surface projection of the lower wing as shown in Fig.1.

AboutTte pressure distribution on the upper wing, on the other hand, the separation bubble along the leading edge made a lower pressure zone for the all wings like a lower wing. However, another lower pressure area was introduced from near the apex of the front-side tapered wing. It is explicit in the streamlines just above the low pressure extension, which is quite similar to that of a delta wing caused by a leading edge separation vortex. The existence of the vortex leads to the C_L performance of the

front-side tapered biplane indicated in Fig.6, which is the same characteristic as a delta wing. Figure16 shows the flow pattern of this front-side tapered biplane at the attack angle of 20 degrees. The vortex and the accompanied low pressure zone were disappeared, and it results in the drop of the lift performance of Fig.6.

This feature of the front-side tapered biplane should come from the flow field generated by the wing with relatively large sweep-back leading edge. Therefore, the laser light sheet method was utilized to assure the vortex behavior. Figure 17 shows the visualization result and a pair of vortices can be seen clearly just on the upper wing of the front-side tapered biplane. Such the vortices could not be seen in the cases of the back-side and the both-side tapered biplanes. The vortices caused the second drastic increase of the lift performance and the sudden drop, namely stall, was observed with the wide spread of the breakdown of the vortices in the case of the front-side tapered biplane. The wind speed was surely reduced from 10m/s to 2m/s for this flow visualization, it is, although, considered that an essential phenomena should be caught by the flow visualization experiment.

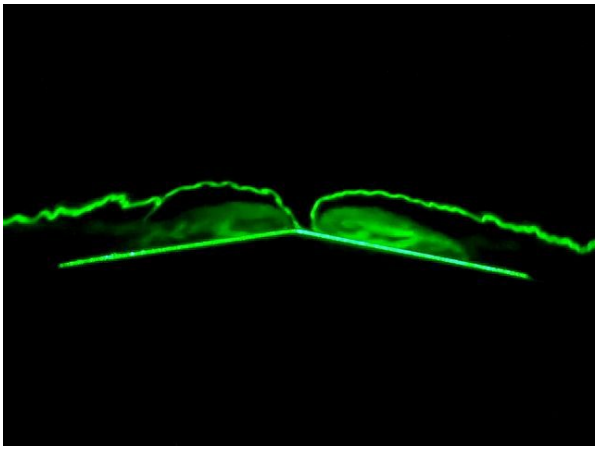

Fig.17 Vortices on the upper wing of the front side tapered biplane.

4 Conclusions

Low speed flight characteristics of three types of a Busemann-type supersonic silent biplane, front-side, rear-side and both-side tapered ones, were investigated by the wind tunnel experiment in the conditions of static and pitching attitude of the biplanes. In the static condition all of the biplanes have the lift performance similar to a general thin wing. However, the result of the front-side tapered biplane at its attack angle higher than eight degrees was different from the others. The reason for the difference is coming from the generation of a leading edge separation vortex on the upper wing of the front-side tapered biplane, which behaves just similar to those of a delta wing including the vortex breakdown.

Under the condition of a pitching flight the all biplanes draw a hysteresis performance with an angle of attack around the static result. These hysteresis characteristics approach closer to the static results in the case of the low frequency pitch motion of 0.5 Hz than the 1.0 Hz results. It comes from the delay of the airflow subordinate to the pitching motion.

Acknowledgement

The authors would like to thank Mr. Yusuke Saito of the Fluid Dynamics Laboratory of the Department of Mechanical and Aerospace Engineering, Tottori University, for his support in the numerical results by the CFD method.

References

[1] Busemann, A., Aerodynamic Lift at Supersonic Speeds, Luftfahrt-forschung, 12th ed., No.6, pp.210-220, 3 Oct.1935.

[2] Liepmann, H.W. and Roshiko, A., Elements of Gas Dynamics, John Wiley & Sons, Inc., New York, pp.107-123, 1957.

[3] http://www.tohoku.ac.jp/japanese/webmagazine /staff/staff_30_obayashi.html

[4] Yamashita, H., Yonezawa, M., Obayashi, S. and Kusunose, K., A Study of Busemann-type Biplane for Avoiding Choked Flow, AIAA Paper, No.2007-0688, 2007.

[5] Maruyama, D., Matsuzawa, T., Kusunose, K. ,Matsushima, K. and Nakahashi, K., Consideration at Off-design Conditions of Supesonic Flows around Biplane Airfoils, AIAA Paper, No.2007-0687, 2007.

[6] Toyoda, A., Okubo, M., Obayashi, S., Shimizu, K., Masuda, A. and Sasoh, A., Ballistic Range Experiment on the Low Sonic Boom Characteristics of Supersonic Biplane, 48th AIAA Aerospace Sciences Meeting Including the New Horizons Forum and Aerospace Exposition, Orlando, FL, 4-7 JAN 2010.

[7] Kuratani, N., Ozaki, S., Obayashi, S., Ogawa, T., Matsuno, T. and Kawazoe, H., Experimental and Computational Studies of Low-Speed Aerodynamic Performance and Flow Characteristics around a Supersonic Biplane, Trans. JSASS, Vol.52, No.176, pp.89-97, 2009.

[8] Ozaki, S., Ogawa, T., Obayashi, S., Matsuno, T. and Kawazoe, H., Evaluation of Three-Dimensional Low-Speed Aerodynamic Performance for a Supersonic Biplane, Trans. JSASS, Vol.57, No.671, pp.461-467, 2009. (in Japanese)

[9] Kawazoe, H. and Morita, S., Ground Effect on the Dynamic Characteristics of a Wing-rock Delta Wing, AIAA Paper, No.2004-2352, pp.1-11, 2004.

Copyright Statement